



Wave-Leak Interaction in a Simple Pipe System

Moez Louati¹; Mohamed S. Ghidaoui, M.ASCE²; Mohamed Mahdi Tekitek³; and Pedro Jose Lee⁴

Abstract: In previous work, the authors have found that blockage-wave interaction relates to Bragg resonance effect, which is governed by the ratio of the wavelength to the length of the blockage. A direct extension of this work for the case of wave-leak interaction has led to a total failure. This is because, unlike blockages, a leak has a vanishingly small length (generally modeled as a point), and according to the blockage results, this would require an infinitesimal wavelength (i.e., infinite frequency). Yet, leak-imposed patterns are known to occur for finite wavelengths. Therefore, the motive of this work was to seek a novel mechanism that is responsible for leak-induced Bragg resonance. It was discovered that what matters in this case is the position of the leak point in relation to the node and antinode of the modes. It is shown that a leak located at an antinode of a given mode will induce Bragg-type resonance of maximum reflection, and the corresponding peak amplitude in the frequency response function (FRF) is a minimum. On the other hand, if a leak is located at a node of a given mode, it experiences Bragg-type resonance of maximum transmission, and the peak amplitude in the FRF is a maximum. The pattern induced by a leak on the FRF, used in many leak detection schemes, is attributable to the leak interaction with different modes. In fact, the closer the leak to a node is, the higher is the amplitude of the corresponding resonant peak, and vice versa for leaks closer to antinodes. A number of leak detection methods are discussed in light of the Bragg resonance mechanism. These insights are exploited for several distinguished leak detection methods showing how a leak-induced pattern is explained from a new point of view. **DOI: 10.1061/(ASCE)HY.1943-7900.0001714.**© 2020 American Society of Civil Engineers.

Author keywords: Bragg resonance; Wave-leak interaction; Frequency response; Pipe system; Transient wave.

Introduction

In the last two decades, various transient-based leak detection methods have been developed and discussed showing promising results. The principle of these techniques is to generate a transient (acoustic) wave in a pipe system [e.g., by rapid maneuver of a valve or a pump, or by using a piezoelectric actuator (Lee et al. 2017)] and analyze the response of the system by measuring the pressure at given location(s). It is important to note that, although some methods use the system response in time domain (e.g., Brunone 1999; Ferrante and Brunone 2003b) and others use the frequency response function (FRF) (e.g., Ferrante and Brunone 2003a; Lee et al. 2005b), the key feature of all of these methods is their reliance on the physics of wave-leak interaction (e.g., Covas et al. 2005; Sattar and Chaudhry 2010). Whether the data are processed in time domain or frequency domain does not change the basic physics,

¹Research Assistant Professor, Dept. of Civil and Environmental Engineering, School of Engineering, Hong Kong Univ. of Science and Technology, Kowloon, Hong Kong (corresponding author). ORCID: https://orcid.org/0000-0003-4661-7164. Email: mlouati@connect.ust.hk

²Chinese Estates Professor of Engineering and Chair Professor, Dept. of Civil and Environmental Engineering, School of Engineering, Hong Kong Univ. of Science and Technology, Kowloon, Hong Kong. Email: ghidaoui@ust.hk

³Associate Professor, Dept. of Mathematics, Univ. of Tunis El Manar, Tunis 1068, Tunisia. Email: mahdi.tekitek@fst.utm.tn

⁴Professor, Dept. of Civil and Natural Resources Engineering, College of Engineering, Univ. of Canterbury, Christchurch 8020, New Zealand. ORCID: https://orcid.org/0000-0001-5282-5758. Email: pedro.lee@canterbury.ac.nz

Note. This manuscript was submitted on July 27, 2018; approved on August 29, 2019; published online on January 27, 2020. Discussion period open until June 27, 2020; separate discussions must be submitted for individual papers. This paper is part of the *Journal of Hydraulic Engineering*, © ASCE, ISSN 0733-9429.

but has an implication on the type and nature of the signal processing applied (Vítkovský and Lee 2008; Covas et al. 2008).

The research focus of transient-based leak detection methods has been on the development of inversion techniques. This led to successful results for simple pipe systems [e.g., reservoir–pipe–valve (RPV) system] (e.g., Wang et al. 2002; Ferrante and Brunone 2003a; Lee et al. 2005a, b; Covas et al. 2005; Ferrante et al. 2007; Sattar and Chaudhry 2010; Gong et al. 2013) and few complex systems (Covas et al. 2005).

Most developed methods make use of the leak-induced resonant peak pattern in the FRF, but an in-depth investigation as to why a leak induces a pattern on the normal modes has not been undertaken. This is a study of the forward problem, in which the physical mechanism of wave-leak interaction in a simple pipe system is investigated to understand the causes of such pattern and its key features. Moreover, an advantage of studying the forward problem is to gather information that could, in return, simplify the inverse problem. In fact, the authors have previously investigated the forward problem of blockage-wave interaction, and showed that it leads to simpler and more accurate detection techniques (Louati et al. 2017).

Previously, the authors have studied the forward problem for the case of blockage-wave interaction (Louati et al. 2018), and showed that it provides insights to simplify the inverse problem (Louati et al. 2017). The mechanism of blockage-wave interaction was related to Bragg resonance effect (Bragg and Bragg 1913; Mei 1985), which is governed by the ratio of the wavelength to the length of the blockage. Many attempts to make a direct extension of this work for the case of wave-leak interaction have led to nonsense results. In fact, a leak has a vanishingly small length (generally modeled as a point), and according to the blockage results, this would require an infinitesimal wavelength (i.e., infinite frequency). Yet, leak-imposed patterns are known to occur for finite wavelengths. Therefore, the motive of this work was to seek a novel mechanism that is responsible for leak-induced Bragg resonance.

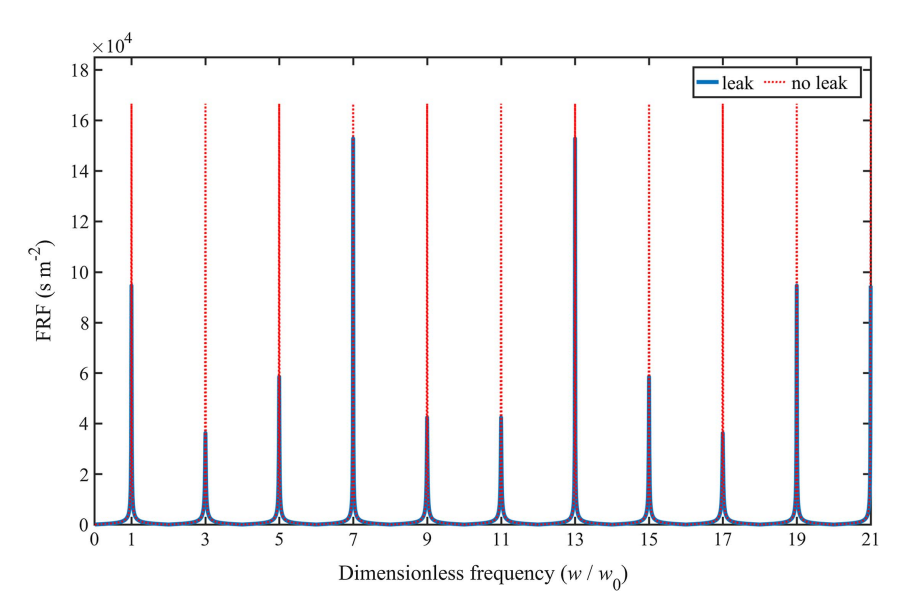


Fig. 1. Comparison between the FRFs of an intact and a leaking RPV system, where a leak is located at $x_l = 1.5/5L$ from the reservoir and measurement taken at the valve location.

To further clarify the objective of this paper, Fig. 1 shows the FRF for a RPV system with a leak located at $x_1 = 1.5/5L$ from the reservoir, where L is the pipe length. The wave is injected at the valve location where the output pressure data are collected. Data in Fig. 1 were obtained using the transfer matrix method (Chaudhry 2014). Therefore, the transient is assumed to be created by an ideal (instantaneous) flow impulse. In Fig. 1, the FRF is the ratio of the output pressure head at the valve to the input flow discharge (generating the transient). The FRF is plotted versus the frequency w normalized by the fundamental resonant frequency of the intact RPV system (w_0) . The dashed curve in Fig. 1 represents the FRF for the case of intact (no leak) pipe system. Fig. 1 shows that the leak induces a variation of the resonant peaks with respect to frequency. Such variation was used by various researchers (e.g., Wang and Ghidaoui 2018; Gong et al. 2013; Sattar and Chaudhry 2010; Lee et al. 2005a, b; Covas et al. 2005; Wang et al. 2002), either explicitly or implicitly, to develop inverse problem algorithms for leak detection.

Lee et al. (2005b) used the leak-induced pattern on the FRF, its periodicity, and its amplitude to develop an elegant method to determine the leak size and location. Moreover, Covas et al. (2005) used what they called *leak resonance* to determine leak locations in pipe systems. Their method is based on observing resonance that is caused by the leak that manifests as high resonant peak in the FRF (see fourth and fifth resonant peaks in Fig. 1). The method developed by Covas et al. (2005) and its equations are obtained by analogy with the electrical cable fault detection method (Maloney 1973). The method shows that the frequency difference between the two high resonant peaks provides the leak location. But why are these resonant peaks of higher magnitudes? Why does the difference in frequency provide information on the leak location? What is causing these variations and what are their features? Moreover, why are different modes damped by the leak differently? Why is the pattern periodic? The objective of this paper was to answer the aforementioned questions and reinterpret leak-induced pattern on the FRF studied in the literature with a new and more explicit point of view.

Bragg-Type Resonance and Governing Equations

The continuity and momentum equation for inviscid and unsteady pipe flow (classical water-hammer equations) are (Ghidaoui 2004)

$$\frac{\partial H}{\partial t} - \frac{a^2}{gA} \frac{\partial Q}{\partial x} = 0$$

$$\frac{\partial Q}{\partial t} - gA \frac{\partial H}{\partial x} = 0$$
(1)

where H = pressure head; Q = flow rate; g = gravitational constant; a = wave speed; and A = pipe area. The convective terms are neglected because the Mach number is of the order of 10^{-3} for most water-hammer applications with typical flow velocities in water supply systems of the order of 1 m s^{-1} , whereas the wave speed is of the order of 1,000 ms⁻¹ (Ghidaoui 2004). Inviscid fluid is considered to simplify the theoretical investigation. In fact, steady friction damps all modes equally. Therefore, the steady friction would not affect the pattern of FRF peaks. However, unsteady friction damps different modes differently. Fortunately, it was found that the unsteady friction interacts minimally with a leak. As a result, the effect of unsteady friction could be subtracted out without any influence on the results (Wang et al. 2002; Nixon et al. 2006; Nixon and Ghidaoui 2007). In addition, the leak-induced signature has been found in laboratory settings where friction is present (Gong et al. 2013; Lee et al. 2006; Ferrante and Bruno 2003a). The waveleak interaction mechanism studied in this work, without accounting for friction, will be applied to experimental examples from the literature, which shows that the effect of friction is not important as long as the leak-induced pattern can be observed.

Fig. 2 shows a semibounded pipe system with a leak, in which the boundary on the right is a reservoir and the boundary on the left

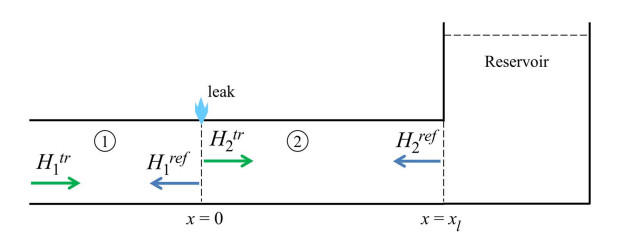


Fig. 2. Semibounded pipe with a leak (the boundary on the left is extended to infinity).

is extended to infinity. Consider a wave train generated by a hydrophone, a hydraulic device, or an acoustic transmitter that propagates in Pipe 1 toward the leak location in Fig. 2. Suppose that this incident wave train has a wave number k, an angular frequency w, and amplitude H_0 . Its form is $H_0 \exp(-ikx + iwt)$, with $i = \sqrt{-1}$. This wave field is governed by the water-hammer equations [Eq. (1)].

Coupling the continuity and momentum equations, the classical water-hammer equation in a frictionless pipe has the following form (Ghidaoui 2004):

$$\frac{\partial^2 H}{\partial t^2} - a^2 \frac{\partial^2 H}{\partial x^2} = 0 \tag{2}$$

Using the method of separation of variables, the solution to Eq. (2) is of the form $\tilde{H}(x,w) \exp(iwt)$, where w and $\tilde{H}(x,w)$ are the radian frequency and the amplitude of the propagating wave in the pipe, respectively. Assume that the pipe system in Fig. 2 is composed of two pipe segments: (1) upstream the leak, and (2) downstream the leak. Therefore, Eq. (2) becomes

$$\frac{d^2 \tilde{H}_j}{dx^2} + k_j^2 \tilde{H}_j = 0; \quad j = 1 \text{ or } 2$$
 (3)

where $k_j = w/a$ is the wave number of the *j*th pipe segment. The solution of Eq. (3) is

$$\tilde{H}_j = H_j^{\text{ref}} \exp(ik_j x) + H_j^{\text{tr}} \exp(-ik_j x) \tag{4}$$

where H_j^{tr} and H_j^{ref} = transmitted and reflected wave amplitudes in pipe j, respectively.

In this case, j = 1 is the pipe section to the left of the leak, and j = 2 is the pipe section to the right of the leak. The conditions of pressure and flow continuity at the leak are

$$\begin{split} \tilde{H}_1 &= \tilde{H}_2 = H_L \\ \tilde{Q}_1 &= \tilde{Q}_2 + Q_L \Leftrightarrow \frac{gA}{iw} \frac{d\tilde{H}_1}{dx} = \frac{gA}{iw} \frac{d\tilde{H}_2}{dx} + s\tilde{H}_2 \quad \text{at } x = 0 \quad (5) \end{split}$$

where H_L and Q_L = pressure head and flow rate at the leak, respectively; and s = leak size. The boundary condition at the reservoir is

$$\tilde{H}_2 = 0 \quad \text{at } x = x_l \tag{6}$$

Eqs. (4)–(6) can be solved for any number of leaks. For simplicity, only the case of single leak (as shown in Fig. 2) is discussed in this work. The extension to multileaks is algebraically involved, but can be performed using software packages, such as MATLAB version R2016b. The case of multiple leaks will be studied in another paper. Assuming no reflections from the upstream boundary (left-hand-side boundary in Fig. 2) and an amplitude of the incident wave H_0 (i.e., $H_1^{\rm tr} = H_0$), Eqs. (4)–(6) give

$$H_{1}^{\text{ref}} + H_{1}^{\text{tr}} = H_{2}^{\text{ref}} + H_{2}^{\text{tr}}$$

$$H_{1}^{\text{ref}} - H_{1}^{\text{tr}} = H_{2}^{\text{ref}} (1 + sZ) - H_{2}^{\text{tr}} (1 - sZ)$$

$$H_{1}^{\text{ref}} \exp(ikx_{l}) + H_{1}^{\text{tr}} \exp(-ikx_{l}) = 0$$

$$H_{1}^{\text{tr}} = H_{0}$$
(7)

which leads to

$$\frac{H_1^{\text{ref}}}{H_0} = \frac{2 + sZ(1 - \exp(2ikx_l))}{-sZ - (2 - sZ)\exp(2ikx_l)}$$
(8)

where

$$Z = a/(gA) \tag{9}$$

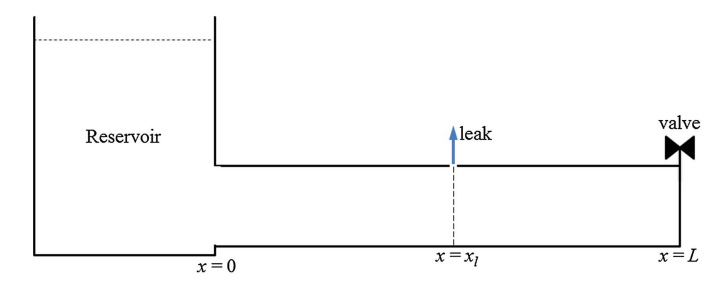


Fig. 3. RPV system with a leak.

Taking the squared norm of the normalized reflection amplitude gives

$$R_c = \left| \frac{H_1^{\text{ref}}}{H_0} \right|^2 = \frac{1 + 2sZ(1 + sZ/2)\sin^2(kx_l)}{1 - 2sZ(1 - sZ/2)\sin^2(kx_l)}$$
(10)

The extrema of the reflected wave amplitude are found if

$$\frac{dR_c}{dk} = \frac{16sZ\cos(kx_l)\sin(kx_l)x_l}{[1 - (2 - sZ)sZ\sin^2(kx_l)]^2} = 0$$
 (11)

Maximum reflection occurs if

$$\cos(kx_l) = 0 \Rightarrow w_n^R(x_l) = 2\pi \left[(2n - 1) \frac{a}{4x_l} \right]; \quad n \in \mathbb{Z}^+ \quad (12)$$

which is precisely Bragg's resonance condition of maximum reflection (Louati et al. 2018; Mei 1985; Bragg and Bragg 1913), where w_n^R = angular frequency at which maximum reflections occur.

Minimum reflection occurs if

$$\sin(kx_l) = 0 \Rightarrow w_n^T(x_l) = 2\pi \left[2(n-1)\frac{a}{4x_l} \right]; \quad n \in \mathbb{Z}^+$$
 (13)

which is precisely Bragg's resonance condition of maximum transmission (Louati et al. 2018; Mei 1985), where w_n^T = angular frequency at which maximum transmissions occur. In the preceding equations, \mathbb{Z}^+ = space on positive integers. Note that maximum reflection occurs when the leak location is an odd multiple of quarter of wavelength [i.e., $x_l = [(2n-1)/4]\lambda$, where λ is the wavelength], and minimum reflection occurs when the leak location is a multiple of half-wavelength [i.e., $x_l = (n/2)\lambda$]. Details on Eqs. (3)–(13) are given in Appendix.

Notice that, if the upstream boundary is changed from being a reservoir (i.e., constant pressure) to a valve (i.e., dead end), then the Bragg resonance conditions are interchanged, in which Eq. (12) becomes the condition of maximum transmission and Eq. (13) becomes the condition of maximum reflection.

The next section shows how the Bragg resonance conditions [Eqs. (12) and (13)] are used to analyze the mechanism of resonant peak variation in the FRF for the case of a bounded RPV system.

Bragg Resonance and Its Relation to Leak-Induced Pattern

This section presents the wave-leak interaction in a bounded pipe system, and discusses how the variation of resonant peaks (especially maximum and minimum resonant peaks) relates to Bragg resonance.

Considering a RPV system with length L and a leak located at $x_l < L$, as shown in Fig. 3. The eigenfrequencies (i.e., natural resonant frequencies) are given by the following dispersion relation (Chaudhry 2014):

$$\cos(k_m L) = 0 \Rightarrow w_m = ak_m = 2\pi \left[(2m - 1)\frac{a}{4L} \right]; \quad m \in \mathbb{Z}^+$$
 (14)

where $k_m = w_m/a$ is the mth wave number; $w_m = m$ th eigenfrequency; and \mathbb{Z}^+ = space on positive integers. The FRF of a RPV system with a leak could be obtained using the transfer matrix method (Chaudhry 2014). The following is the FRF (which is represented as Υ) for the case of a frictionless pipe measured at a given location x_M along the pipe system:

$$\Upsilon = \frac{M_{u-x_M}}{M_{u-d}} \tag{15}$$

where

$$\begin{cases}
M_{u-x_{M}} = \begin{cases}
-iZ\sin(kx_{M}) & \text{if } x_{M} \leq x_{l} \\
i\cos(kx_{l})\sin(k(x_{M} - x_{l})) \\
-Z \begin{bmatrix} i\cos(kx_{l})\sin(k(x_{M} - x_{l})) \\
+i\sin(kx_{l}) \begin{pmatrix} \cos(k(x_{M} - x_{l})) \\
+i(Z/Z_{L})\sin(k(x_{M} - x_{l})) \end{pmatrix} \end{bmatrix} & \text{if } x_{M} \geq x_{l} \\
M_{u-d} = \cos(kx_{l})\cos(k(L - x_{l})) + i\sin(kx_{l}) \begin{bmatrix} i\sin(k(L - x_{l})) \\
+(Z/Z_{L})\cos(k(L - x_{l})) \end{bmatrix}
\end{cases}$$
(16)

 $Z_L = (2\bar{H}_L/\bar{Q}_L)$ is the impedance at the leak; and \bar{H}_L and \bar{Q}_L = mean pressure head and mean flow rate at the leak, respectively. The squared magnitude of the FRF is

$$|\Upsilon|^{2} = \frac{[Z\sin(kx_{M})]^{2}}{\cos^{2}(kL) + (Z/Z_{L})^{2}\sin^{2}(kx_{l})\cos^{2}(k(L-x_{l}))} \quad \text{if } x_{M} \le x_{l}$$

$$|\Upsilon|^{2} = \frac{(Z_{c}^{0})^{2}[\sin^{2}(kx_{M}) + (Z/Z_{L})^{2}\sin^{2}(kx_{l})\sin^{2}(k(x_{M}-x_{l}))]}{\cos^{2}(kL) + (Z/Z_{L})^{2}\sin^{2}(kx_{l})\cos^{2}(k(L-x_{l}))} \quad \text{if } x_{M} \ge x_{l}$$

$$(17)$$

It is highly instructive to impose Bragg resonance conditions [Eqs. (12) and (13)], derived in the previous section on the FRF [Eq. (17)]. This allows studying the relation between Bragg resonance conditions and the variation of the mode amplitudes at the eigenfrequencies observed in a FRF of a pipe system with a leak. To relate the Bragg resonance frequencies to the eigenfrequencies of the system, Eq. (14) is imposed, such that the Bragg resonance conditions [Eqs. (12) and (13)] become, respectively

$$w_m = w_n^R(x_l) \Rightarrow \frac{x_l}{L} = \frac{2n-1}{2m-1}$$
 (18)

and

$$w_m = w_n^T(x_l) \Rightarrow \frac{x_l}{L} = \frac{2n}{2m-1} \tag{19}$$

Eqs. (18) and (19) correspond to the leak locations where Bragg resonance of maximum reflection and minimum reflection occurs at a given mode m, respectively. Notice that the locations in Eqs. (18) and (19) also correspond to the locations of stagnation points (i.e., maximum pressure or zero flow) and pressure nodes (zero pressure or maximum flow) of a given mode m. The physical interpretation of these locations and their implications is discussed next.

In the following sections, only a RPV system is considered, but if the system has symmetric boundary conditions, such as reservoir– pipe–reservoir (RPR) or valve–pipe–valve (VPV), the study of the effect of Bragg resonance on the FRF leads to the same conclusions with the following changes in the Bragg resonance conditions:

· Bragg resonance condition of maximum reflection

RPR system:
$$\begin{cases} w_n^R = 2\pi \left[(2n-1) \frac{a}{4x_l} \right]; & n \in \mathbb{Z}^+ \\ \frac{x_l}{L} = \frac{2n-1}{2m} \end{cases}$$
 (20)

VPV system:
$$\begin{cases} w_n^R = 2\pi \left[2(n-1)\frac{a}{4x_l} \right]; & n \in \mathbb{Z}^+ \\ \frac{x_l}{L} = \frac{(n-1)}{m} \end{cases}$$
 (21)

· Bragg resonance condition of maximum transmission

RPR system:
$$\begin{cases} w_n^T = 2\pi \left[2(n-1)\frac{a}{4x_l}\right]; & n \in \mathbb{Z}^+\\ \frac{x_l}{L} = \frac{(n-1)}{m} \end{cases}$$
 (22)

VPV system:
$$\begin{cases} w_n^T = 2\pi \left[(2n-1) \frac{a}{4x_l} \right]; & n \in \mathbb{Z}^+ \\ \frac{x_l}{L} = \frac{2n-1}{2m} \end{cases}$$
 (23)

It is important to note that, if the pipe system boundaries are unknown, then the Bragg resonance conditions cannot be determined. In addition, if the boundaries of the system consist of partially opened or partially closed valves, then they should be either known or determined to obtain the Bragg resonance conditions. According to the work of Wylie and Streeter (1993), which was further discussed by Tijsseling and Vardy (2017), partially opened/closed valves behave as fully opened or fully closed valves depending on the degree of opening. For example, if the opening of the downstream valve in Fig. 3 is more than 50%, then it behaves as fully opened, which means the resonant frequency will be even numbered (similar to the RPR system). If the valve is less than 50% opened, then the system responds similarly to the RPV system (which means the resonant frequencies will be odd numbered). Other boundary conditions can be analyzed by changing Eq. (6) and the third line in Eq. (7).

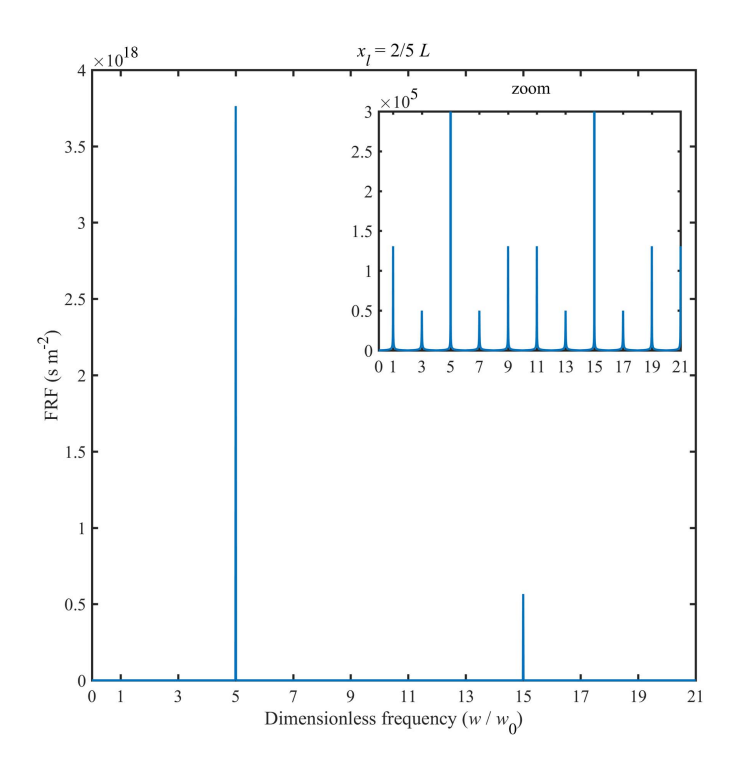


Fig. 4. FRF for a RPV system with a leak located at 2/5L and measurement taken at $x_M = L$ (at the valve) using the transfer matrix method.

Effect of Bragg Resonance Condition of Maximum Transmission on the FRF

Inserting Eqs. (14) and (19) into Eq. (17) gives

$$|\Upsilon|^2 = \frac{\left[Z\sin\left(n\pi\frac{x_M}{x_l}\right)\right]^2}{\cos^2((2m-1)\frac{\pi}{2})} \quad \text{if } x_M \le x_l$$

$$|\Upsilon|^2 = \frac{\left[Z\sin\left(n\pi\frac{x_M}{x_l}\right)\right]^2}{\cos^2((2m-1)\frac{\pi}{2})} \quad \text{if } x_M \ge x_l$$
(24)

Eq. (24) shows that the FRF tends to infinity unless the numerator is zero. Note that the FRF approaches infinity only for the case of inviscid flow. Of course, in reality, the amplitude would not become infinite because of the presence of friction. For example, if measurement is taken at the valve $(x_M = L)$, Eq. (24) becomes $|\Upsilon| = Z/\cos[(2m-1)(\pi/2)] \to \infty$. The reason for the amplitude to tend to infinity is because, at this specific mode m, in which Bragg resonance of minimum reflection is satisfied, the leak is located at a pressure node (zero pressure) of the mth harmonic. (This is discussed further in the next section.) Therefore, the pipe system with a leak behaves similarly to an intact pipe system at mode m that satisfies Bragg resonance of maximum transmission. At this mode, Eq. (19) is satisfied, implying minimum reflection. Moreover, the FRF form in Eq. (24) is the same as the FRF for an intact frictionless pipe system. Fig. 4 shows the FRF for the case of a RPV system with a leak located at $x_l = 2/5L$, which satisfies Eq. (19) with m = 3 and n = 1, and measurement taken at $x_M = L$. Fig. 4 shows that, at the third eigenfrequency, the amplitude is infinite (i.e., very large) as expected. Such behavior occurred in a previous literature, and some examples will be discussed later in this paper. Fig. 4 is a zoomed picture that shows that the FRF at other eigenfrequencies is not zero, but simply much smaller.

It is interesting to note that, if measurement is taken at a distance that is a multiple of the leak location $(x_M = jx_l; j \in \mathbb{Z}^+)$, the FRF becomes zero [Eq. (24)]. For example, if $x_M = 2x_l$, then $|\Upsilon| \to 0$.

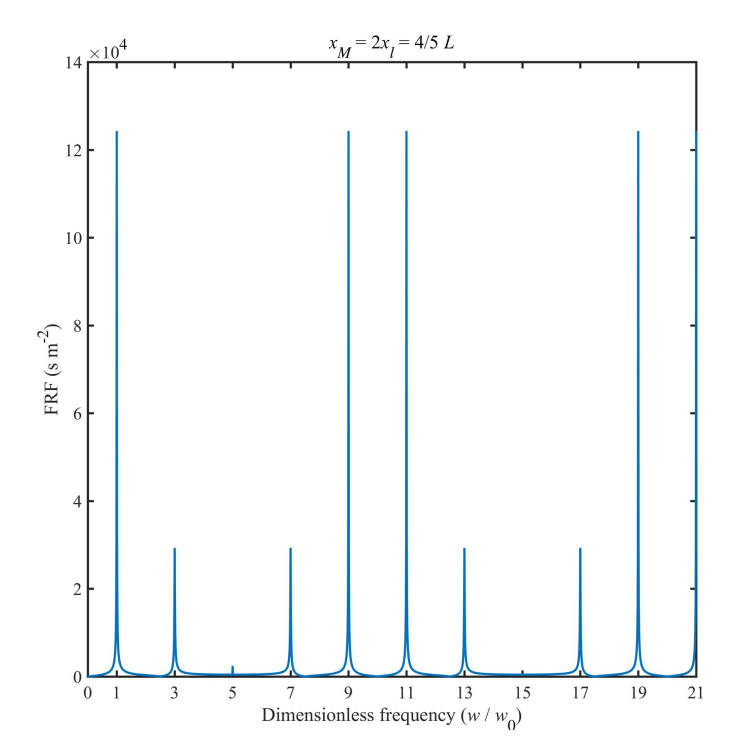


Fig. 5. FRF for a RPV system with a leak located at $x_l = 2/5L$ and measurement taken at $x_M = 2x_l = 4/5L$.

The reason for such behavior is that, if the leak is located at a pressure node, then a measurement at a multiple distance of the leak will also be at a pressure node where the pressure amplitude is zero. Fig. 5 shows the FRF for the case of a RPV system with a leak located at $x_l = 2/5L$, which satisfies Eq. (19) with m = 3 and n = 1, and measurement taken at $x_M = 2x_l$. Fig. 5 shows that, at the third eigenfrequency, the amplitude is *zero* as expected. Therefore, measurement location is an important parameter.

Effect of Bragg Resonance Condition of Maximum Reflection on the FRF

In this section, the Bragg resonance condition of maximum reflection is considered by inserting Eqs. (14) and (18) into Eq. (17), which gives

$$|\Upsilon|^2 = \left[Z_L \sin\left((2n - 1) \frac{\pi}{2} \frac{x_M}{x_l} \right) \right]^2 \quad \text{if } x_M \le x_l$$

$$|\Upsilon|^2 = \left[Z_L \sin\left((2n - 1) \frac{\pi}{2} \frac{x_M}{x_l} \right) \right]^2$$

$$+ \left[Z \cos\left((2n - 1) \frac{\pi}{2} \frac{x_M}{x_l} \right) \right]^2 \quad \text{if } x_M \ge x_l$$
(25)

Eq. (25) shows that the FRF gives a finite value and has two particular cases. The first case is when $\cos[(2n-1)(\pi/2)(x_M/x_I)] = 0$, which implies that the measurement location satisfies a *similar* condition as the Bragg resonance of maximum reflection in Eq. (18) [i.e., $x_I/x_M = (2n-1)/(2n'-1)$, with n' a positive integer]. This means that the measurement location is at a maximum pressure point. In this case, the magnitude of FRF at that particular mode m is equal to the leak impedance. For example, if $x_M = L$, which satisfies Bragg's condition in Eq. (18), the FRF gives $|\Upsilon| = Z_L$ at mode m. In fact, at Bragg resonance condition of maximum reflection [Eq. (18)], the leak is located at a maximum pressure point of the mth harmonic. (This is discussed further in the next section.) Under such condition, the flow across

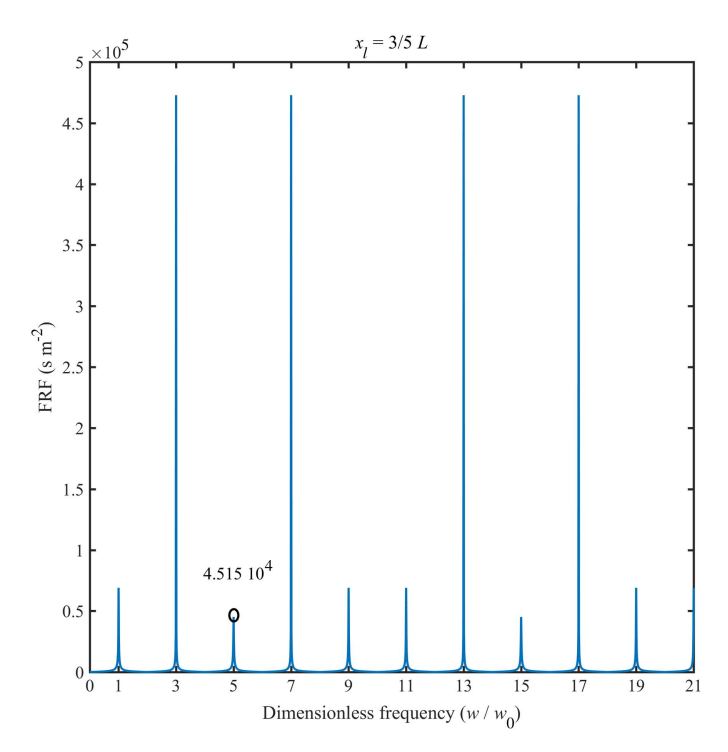


Fig. 6. FRF for a RPV system with a leak located at 3/5L and measurement taken at $x_M = L$ (at the valve).

the leak is maximum, and therefore, the effect of the leak is also maximum. (The amplitude of the mth mode is therefore highly attenuated.) By consequences, the reflection from the leak is maximum. When the measurement location is also at a maximum pressure of mode m, the measurement records exactly what occurred at the leak for mode m. Therefore, by measuring at the valve, the size of a leak can be determined (approximatively) by identifying the minimum amplitude that gives the leak impedance (Z_L = $2\bar{H}_L/\bar{Q}_L$). Fig. 6 shows the FRF for the case of a RPV system with a leak located at $x_l = 3/5L$, which satisfies Eq. (18) with m = 3and n = 2, and measurement taken at $x_M = L$. The characteristics of the leak used to obtain Fig. 6 are leak size $s = 5 \times 10^{-5}$ m², the flow at the leak $\bar{Q}_L = s\sqrt{2g\bar{H}_L}$, and $\bar{H}_L = H_0 = 25$ m. Fig. 6 shows that, at the third eigenfrequency, the amplitude is minimum as expected, and the value of the amplitude corresponds to the leak impedance ($Z_L = 2\bar{H}_L/\bar{Q}_L = 4.515\,10^4~\mathrm{s\,m^{-2}}$). In fact, this property is implicitly used in Wang et al. (2002) and it is discussed in detail later in this paper.

The second case observed in Eq. (25) is when $\sin[(2n-1)(\pi/2)(x_M/x_l)] = 0$, which implies that the measurement location satisfies a *similar* condition as the Bragg resonance of maximum reflection for the case of RPR in Eq. (20) [i.e., $x_l/x_M = (2n-1)/(2n')$], where n' is a positive integer. This means that the measurement location is at the pressure nodes of the RPR harmonics. This condition is actually similar to the first case condition, but for the cases in which the maximum damping occurs at the antiresonant frequencies. In this case, the magnitude of the FRF at that particular mode m is equal to the pipe impedance. For example, if $x_M = 2x_l$, the FRF gives $|\Upsilon| = Z$ at mode m.

Mechanism of Resonant Peak Variations and Its Properties

Having understood the relation between the FRF peak variation, the leak-mode interaction, and Bragg resonance effect, one could describe the following mechanism: when transient waves are generated into a pipe with a leak located at a given location x_l , the harmonic modes are excited. These harmonic modes (or standing waves) have pressure nodes (where the transient pressure is zero) and stagnation points (or antinodes where the transient pressure is maximum). If the leak is located at or near a pressure node of mode m, then the mth resonance peak observed in the FRF would have a maximum (or very large) value. On the other hand, if the leak is located at or near a stagnation point of mode m, then the mth resonance peak observed in the FRF would have a minimum (or very small) value. The leak location at either stagnation point or pressure node is related to Bragg resonance of maximum or minimum reflection, respectively, as discussed in previous sections. If the leak is located in neither stagnation point nor pressure node of mode m, then the mth resonance peak observed in the FRF would have an intermediate value (between the minimum and maximum values). Fig. 7 is a sketch of three different leak locations and how the mth resonant peak varies accordingly (m = 3 in Fig. 7).

Another property of the FRF is that the resonant peak variations observed are periodic, and the reason is because the Bragg resonance effect is also periodic. In fact, if Bragg resonance is observed at mode m_0 , the other similar Bragg resonances are observed at mode m_2 , where $2m_2-1$ is an odd multiple of $2m_0-1$ for a RPV system [Eqs. (26) and (27)]

$$\frac{w_n^R}{w_0} = (2n - 1)\frac{L}{x_l} = \underbrace{\frac{(2n - 1)}{(2n_0 - 1)}}_{\text{odd}}\underbrace{(2m_0 - 1)}_{\text{odd}} = \underbrace{(2m_2 - 1)}_{\text{odd}}; \quad n \in \mathbb{Z}^+$$
(26)

$$\frac{w_n^T}{w_0} = 2(n-1)\frac{L}{x_L} = \underbrace{\frac{(n-1)}{(n_0-1)}}_{\text{must be odd}}\underbrace{(2m_2-1)}_{\text{odd}} = \underbrace{(2m_2-1)}_{\text{odd}}; \quad n \in \mathbb{Z}^+$$
(27)

Therefore, an intermediate resonant peak [Figs. 7(e and f)] at a given mode m_i is observed again at mode m_{i2} , where $m_{i2} = m_i + 2(m_2 - m_i)$.

Revisiting the Literature in Light of the Bragg Resonance Mechanism

Note that, so far, only a RPV system is considered, but if the system has symmetric boundary conditions, such as RPR or VPV, the previously described mechanism still holds with the following changes in periodicity property of the FRF and Bragg resonance effect:

· Bragg resonance condition of maximum reflection

RPR system:
$$\frac{w_n^R}{w_0} = (2n - 1) \frac{L}{x_l}$$
$$= \underbrace{\frac{(2n - 1)}{(2n_0 - 1)}}_{\text{odd}} \underbrace{(2m_0)}_{\text{even}} = \underbrace{(2m_2)}_{\text{even}}; \quad n \in \mathbb{Z}^+$$
(28)

VPV system:
$$\frac{w_n^R}{w_0} = 2(n-1)\frac{L}{x_l}$$

$$= \underbrace{\frac{(n-1)}{(n_0-1)}}_{\text{even}} \underbrace{(2m_0)}_{\text{even}} = \underbrace{(2m_2)}_{\text{even}}; \quad n \in \mathbb{Z}^+$$
(29)

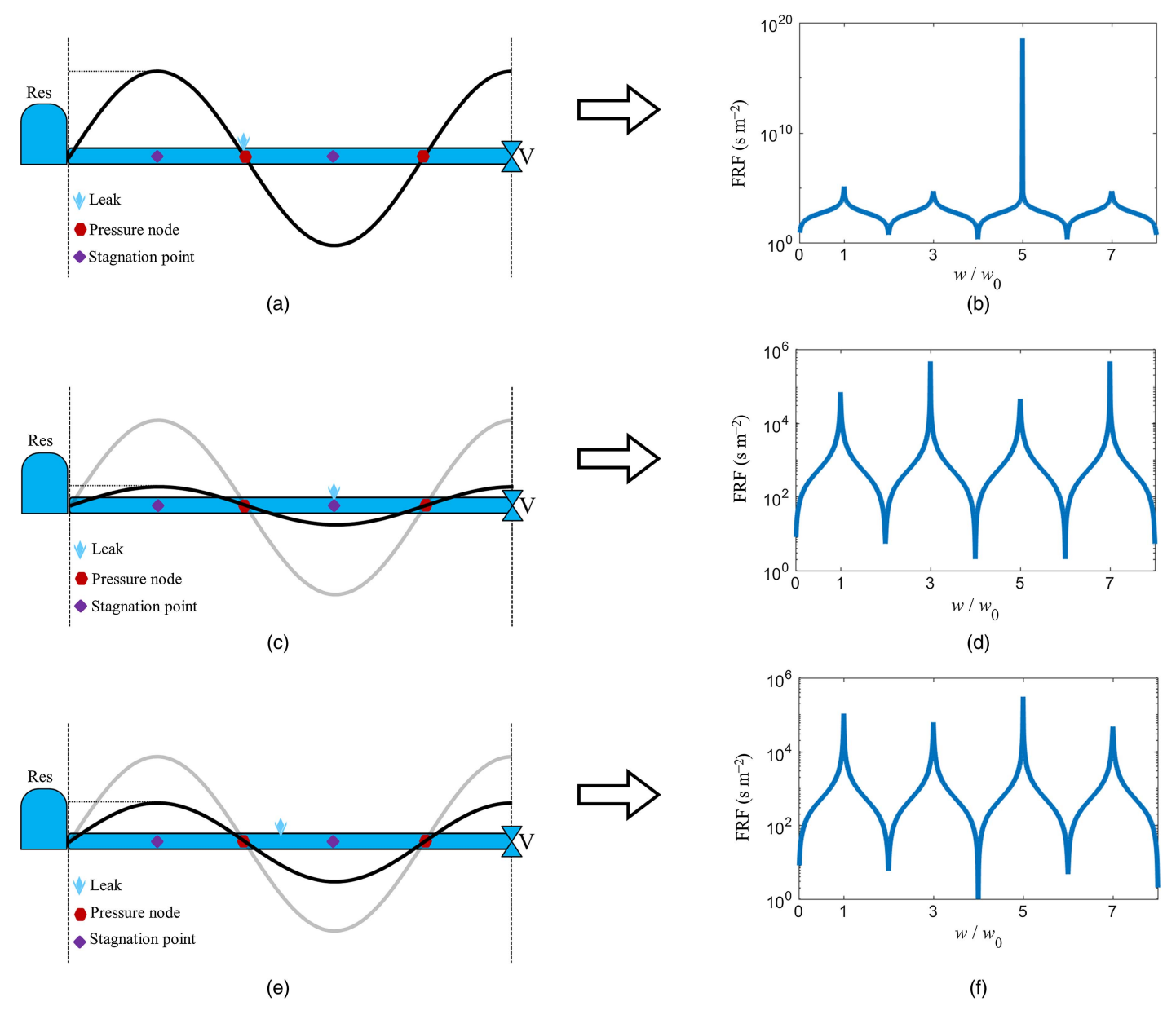


Fig. 7. Mechanism of FRF peak pattern: (a and b) defect at a pressure node of the third harmonic; (c and d) defect at a stagnation point of the third harmonic; and (e and f) defect is at an intermediate location.

Bragg resonance condition of maximum transmission

RPR system:
$$\frac{w_n^T}{w_0} = 2(n-1)\frac{L}{x_l}$$

$$= \underbrace{\frac{(n-1)}{(n_0-1)}}_{\text{odd or even}} \underbrace{(2m_0)}_{\text{even}} = \underbrace{(2m_2)}_{\text{even}}; \quad n \in \mathbb{Z}^+ \quad (30)$$

VPV system:
$$\frac{w_n^T}{w_0} = (2n-1)\frac{L}{x_l}$$

$$= \underbrace{\frac{(2n-1)}{(2n_0-1)}}_{\text{even}}\underbrace{(2m_0)}_{\text{even}} = \underbrace{(2m_2)}_{\text{even}}; \quad n \in \mathbb{Z}^+$$
 (31)

Relation of Bragg Resonance to the Method by Wang et al. (2002)

Bragg resonance of maximum reflection shows that, if leaks are located at stagnation points [Eqs. (18), (20), and (21)], then particular modes are damped severely. Fig. 9(c) in Wang et al. (2002) points out that the second mode is extremely damped because of the leak in comparison with the other modes. This fact can now be understood by Bragg resonance. In particular, the leak location considered in Wang et al. (2002) is $x_l = 1/4L$, which satisfies Eq. (20) with m=2 and n=1 for a RPR system. In fact, the following damping equation is introduced in Wang et al. (2002):

$$R_{mL} = \overline{A_L} \sin^2(m\pi x_l/L) \tag{32}$$

where $\overline{A_L}$ = modified leak size; and $\sin(m\pi x_l/L)$ = normalized harmonic function for a RPR system, which clearly shows that the damping caused by a leak is proportional to the squared normalized

magnitude of the *m*th harmonic. As the harmonic function decreases, the damping caused by the leak decreases; hence, the effect of the leak is weaker. Therefore, the resonant peak is higher. As a result, the variation of the resonant peaks is *inversely* proportional to the damping magnitude.

Wang et al. (2002) derived their equation for a RPR and, when they applied it for RPV, they had to create a fictitious symmetric RPV system to go back to their original RPR system. However, it can be shown that the same conclusion holds for a RPV system, in which the damping function becomes

$$R_{mL} = \overline{A_L} \sin^2 \left((2m - 1) \frac{\pi x_l}{2L} \right)$$
 (33)

If Eq. (33) is used for the RPV system case in Wang et al. (2002) taking the damping ratio between modes m = 2 and m = 1, it gives $x_l = 0.24L$, as found by adding the fictitious second RPV system. In fact, the solution is unique as stated in Wang et al. (2002). This uniqueness can be shown explicitly from the new point of view of Bragg resonance. In the case of Wang et al. (2002), the uniqueness comes from the fact that the ratio of the harmonic magnitudes between modes m = 2 and m = 1 is unique when $x_l = 0.25L$, as shown in Fig. 8(a). In other words, there is no other location along the pipe where the ratio of the harmonic magnitudes between modes m=2 and m=1 is the same as at the location 0.25L [Fig. 8(a)]. However, for the case of the RPR system, Fig. 8(b) shows that the ratio of the harmonic magnitudes between the first three harmonics in the RPR system is equal at two locations ($x_l = 0.25L$ and $x_l =$ 0.75L), which makes the solution nonunique as found in Wang et al. (2002). Note that, if the ratio between the third and second harmonics of the RPV system is taken instead of the second and first harmonics, then the solution will be nonunique similar to the RPR system [Fig. 8(a)]. This is because the ratio of the harmonic magnitudes between modes m=3 and m=2 is the same at two locations ($x_l=0.25L$ and $x_l=0.75L$), as shown in Fig. 8(a). In addition, it is clear from Fig. 8(a) that, for the case of the RPV system, the second harmonic leads to much higher damping than the first harmonic, because its magnitude is higher at $x_l=0.25L$. The large damping is shown in Wang et al. (2002).

Relation of Bragg Resonance to the Analysis Work by Ferrante and Brunone (2003a)

While studying the effect of leak impedance on FRF, Ferrante and Brunone (2003a) analyzed the impedance function. They found special conditions at which the impedance measured at the downstream boundary goes to *infinity* (for an ideal frictionless pipe). These conditions [Eqs. (38) and (41) in Ferrante and Brunone (2003a)] correspond to the Bragg resonance conditions of maximum transmission. Although Ferrante and Brunone (2003a) studied the case of RPV, their Eq. (41) corresponds to the condition of Bragg resonance of maximum transmission for the case of RPR. The reason is that Eq. (41) provides the condition on FRF at the antiresonant frequencies, which behaves precisely the same as the FRF at the resonant frequencies for a RPV case.

In addition, Ferrante and Brunone (2003a) provided a condition in their Eq. (33), which is not related to Bragg resonance, but for consistency, Eq. (17) is rewritten as follows (with $x_M = L$) to show that such condition occurs in addition to Bragg resonance conditions:

$$|\Upsilon|^2 = Z^2 \tan^2(kL) \frac{1 + \frac{1}{4}(Z/Z_L)^2 \sin^2(2kx_l) [1 - \cot(kL) \tan(kx_l)]^2}{1 + \frac{1}{4}(Z/Z_L)^2 \sin^2(2kx_l) [\tan(kL) - \tan(kx_l)]^2}$$
(34)

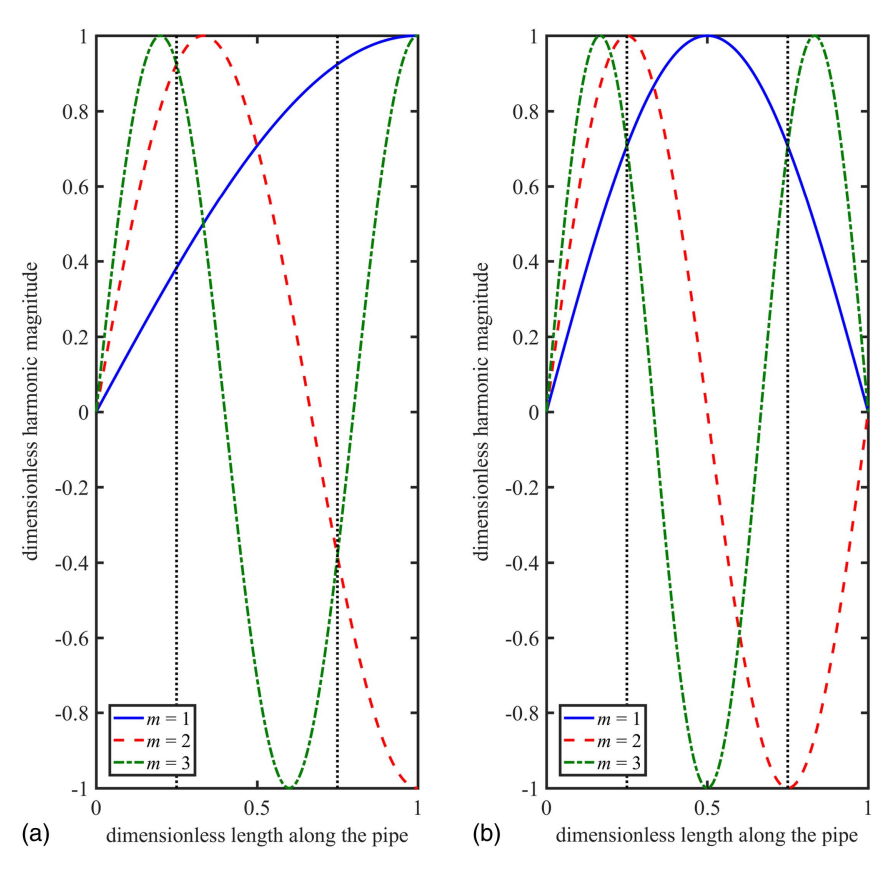


Fig. 8. Dimensionless harmonic magnitude for the first three modes: (a) RPV system; and (b) RPR system.

Bragg resonance conditions are governed by $\sin(2kx_l) = 2\sin(kx_l)\cos(kx_l) = 0$. For example, Bragg resonance of maximum transmission occurs when $\sin(kx_l) = 0$ [Eq. (13)], and Eq. (17) reduces to $|\Upsilon|^2 = Z^2 \tan^2(\gamma L)$, which is the FRF for the intact pipe case. If

$$\tan(kL) = \tan(kx_l) \tag{35}$$

Eq. (17) reduces also to $|\Upsilon|^2 = Z^2 \tan^2(\gamma L)$. The frequencies at which Eq. (35) is satisfied do not correspond to the fundamental resonance frequencies. This condition actually corresponds to the intersection of the asymptotic cases of the RPV system with leak. At the asymptotic (extreme) case, where the leak is large enough to behave as a reservoir, the RPV system with leak decouples into a RPR and RPV system with length x_l and $1 - x_l$, respectively. The FRFs of different leak cases intersect at the intersection of the intact case and decoupled case asymptotes. A more detailed analysis on the condition in Eq. (35) will be discussed in another paper.

Relation of Bragg Resonance to the Methods by (Lee et al. 2005a, b)

Lee et al. (2005b) exploited the periodicity property of FRF discussed previously (section "Mechanism of Resonant Peak Variations and Its Properties") and the proportionality effect between the wave-leak interaction and the resonant peaks to locate leaks in a pipe system. Lee et al. (2005b) first inverted the values of the resonant peaks, which become proportional to the harmonic function, and by applying discrete Fourier transform (DFT), the leak location is determined. Note that the DFT gives the period at which the harmonic function becomes maximum or minimum. Eq. (33) [or Eq. (32)] shows that the maximum and minimum damping obey the Bragg resonance conditions [Eqs. (12) and (13)].

The maximum and minimum damping effects governed by Bragg resonance appear in the results by Lee et al. (2005b). For example, Fig. 1 in Lee et al. (2005b) clearly shows that the peak of the seventh harmonic is very large (about the same as the peak for the no leak case). This fact can be explained by Bragg resonance. In particular, the leak is located at a pressure node, where $x_l = 0.15L$, which is approximately 2/13L. This corresponds to the case, where m = 7 and n = 1 in Eq. (19). At this location, Bragg resonance of maximum transmission occurs and the effect of the leak becomes very weak. This is why the leak and no leak cases coincide at the seventh harmonic shown in Fig. 1 by Lee et al. (2005b). Similar interpretations can be given for the experimental results in Lee et al. (2006). For example, Fig. 17 in Lee et al. (2006) shows that, for a RPV system, the fourth mode experiences large damping when the leak location is at about $x_l = 0.75L$ away from the reservoir. This is very close to the pressure antinode of the fourth mode, and thus, it experiences Bragg resonance of maximum reflection with m = 4 and n = 3 [Eq. (18)]. On the other hand, the second and sixth modes experience little damping because the leak is located near the pressure nodes of the second and sixth modes, and thus, they experience Bragg resonance of maximum transmission with (m = 2 and n = 1) and (m = 6 and n = 4), respectively. This experimental example shows that the effect of friction does not affect the mechanism of wave-leak interaction.

Another interesting leak detection method that also uses the mechanism of wave-leak interaction described previously is the peak sequencing method by Lee et al. (2005a). In this method, Lee et al. (2005a) relaxed their need of using the periodicity property of the FRF. However, this method does not determine the leak location, but gives a range where the leak location could be. The range becomes narrower (better accuracy) if more resonant peaks

are used. The peak sequencing method recognizes the sequence of which resonant peak is higher than the other, sorts the sequence from highest to lowest, and then finds the corresponding range of leak location where the harmonic amplitudes are sequenced and sorted from lowest to largest [because they are inversely proportional, as discussed previously throughout the methods by Wang et al. (2002)]. The work by Lee et al. (2005a) is perhaps the closest of all leak detection methods to indicate the link between the harmonics and leak location, because it uses the information that higher amplitude of a harmonic at the leak location would induce lower amplitude of the FRF peak. However, in their paper, they neither explain nor discuss the full physical mechanism of leakharmonic interaction. The current work gives full details on the leak-harmonic interaction and their relation to Bragg-type resonance. In fact, Bragg resonance shows that the variation of the resonant peaks of FRF is inversely proportional to the variation of the harmonic amplitude at the leak location: the lower the resonant peak is, the higher is the amplitude of the harmonic at the leak location, and vice versa for higher resonant peak values. Combining the knowledge of possible leak locations obtained from the Bragg resonance effect with the peak sequencing method could lead to a much narrower leak location range (better accuracy) without using a larger number of resonant peaks.

Relation of Bragg Resonance to the Method by Covas et al. (2005)

Covas et al. (2005) introduced a leak detection method, in which they used the properties of Bragg resonance effect and the periodicity property. Unlike Lee et al. (2005b), who performed Fourier transform on the resonant peaks, Covas et al. (2005) applied Fourier transform on the whole FRF. In fact, Covas et al. (2005) appear to be the first to exploit leak resonance modes. Their equation of leak resonance is obtained from analogy with electrical system to determine the cable fault location (Maloney 1973). The current work shows that this resonance is attributable to Bragg resonance effect. Covas et al. (2005) used the difference in frequency between two consecutive Bragg resonances of maximum transmission to determine the leak location. In Fig. 6 from Covas et al. (2005), the first resonance occurred at the third harmonic, which is because the leak is located at $x_l = 0.8L = 4/5L$. [Note that, in Covas et al. (2005), x_l is measured from the valve; here, x_l is measured from the reservoir.] This corresponds to the case, where m=3 and n=2 in Eq. (19). The second resonance occurred at m=8 because it also satisfies Eq. (19) when n=4. It is important to state that Bragg resonance shows that the leak resonance can occur at the same mode numbers if the leak is at $x_l = 0.4L =$ 2/5L instead of $x_l = 0.8L = 4/5L$. Fig. 9 gives the FRFs for the two leak locations ($x_l = 2/5L$ and $x_l = 4/5L$). Fig. 9 shows that, for both cases, the leak resonance [as called in Covas et al. (2005)] occurs at the same modes. The FRFs are distinguished by looking at the lower resonant peaks that occur at different modes. For the case, in which $x_l = 2/5L$, the first low resonant peak occurs at Mode 2. The reason for this mode to damp the amplitude largely is because it is close to a maximum pressure position. In fact, it nearly satisfies Eq. (18) for Bragg resonance of maximum reflection with m = 2 and n = 1. However, for the case $x_1 = 4/5L$, the lower resonant peak occurs at Mode 4. The reason for this mode to damp the amplitude largely is because it is close to a maximum pressure position. In fact, it nearly satisfies Eq. (18) for Bragg resonance of maximum reflection with m = 4 and n = 3.

It is shown in the section "Effect of Bragg Resonance Condition of Maximum Transmission on the FRF" that the measurement locations could modify the FRF severely; therefore, it is important to

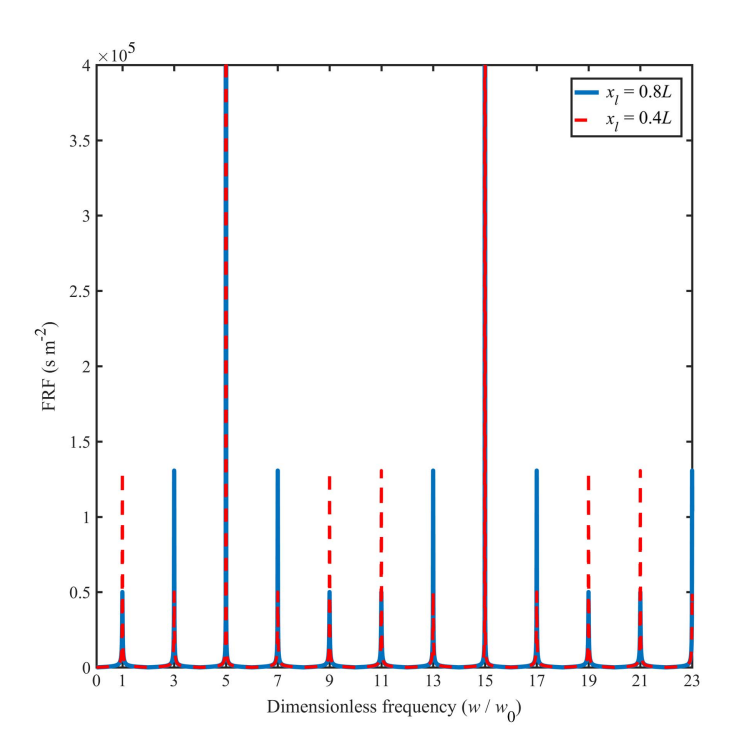


Fig. 9. Comparison of the FRFs of the RPV system with measurement at $x_M = L$ and a leak at $x_l = 4/5L$ and $x_l = 2/5L$. (Data from Covas et al. 2005.)

take such information into account. In fact, using the FRF in Fig. 5 to obtain the frequency difference between the leak resonant peaks, as applied in Covas et al. (2005), will lead to an error. For example, Fig. 5 shows that the resonant peaks at Modes 5 and 6 are large, and the dimensionless frequency difference is $\Delta w_R^* = 2$. In this case, Eq. (16) in Covas et al. (2005) gives $x_l = 0$. [Note that, in Covas et al. (2005), x_l is measured from the valve; here, x_l is measured from the reservoir.] Fig. 5 also shows that it is possible to take the frequency difference between Modes 6 and 10, which is $\Delta w_R^* = 8$. In this case, Eq. (16) in Covas et al. (2005) gives $x_l = 0.75$. The errors are because the true *large* resonant peaks corresponding to the leak resonance (or Bragg resonance of maximum transmission) become very small because of the change of measurement location.

Relation of Bragg Resonance to the Method by Sattar and Chaudhry (2010)

Another interesting aspect of the wave-leak interaction is that the Bragg resonance does not affect the resonant peaks only, but, in fact, it affects the antiresonant peaks as well in a very similar way. Actually, the antiresonant peaks are simply the resonant peaks for a symmetric RPR system, as shown in Fig. 10. This means that the same information that could be extracted from the resonant peaks could also be extracted from the antiresonant peaks. For example, $x_1 = 3/5L$ satisfies the Bragg resonance condition of maximum reflection for a RPV system [Eq. (18)] with m = 3 and n = 2, but it also satisfies the Bragg resonance condition of maximum transmission for a RPR system [Eq. (22)] with m = 5 and n = 3. This is precisely the information that is used implicitly for the leak detection method by Sattar and Chaudhry (2010). Similar to the methods by Covas et al. (2005) and Lee et al. (2005b), Sattar and Chaudhry (2010) used the leak-induced pattern on the antiresonant peaks to develop a leak detection method.

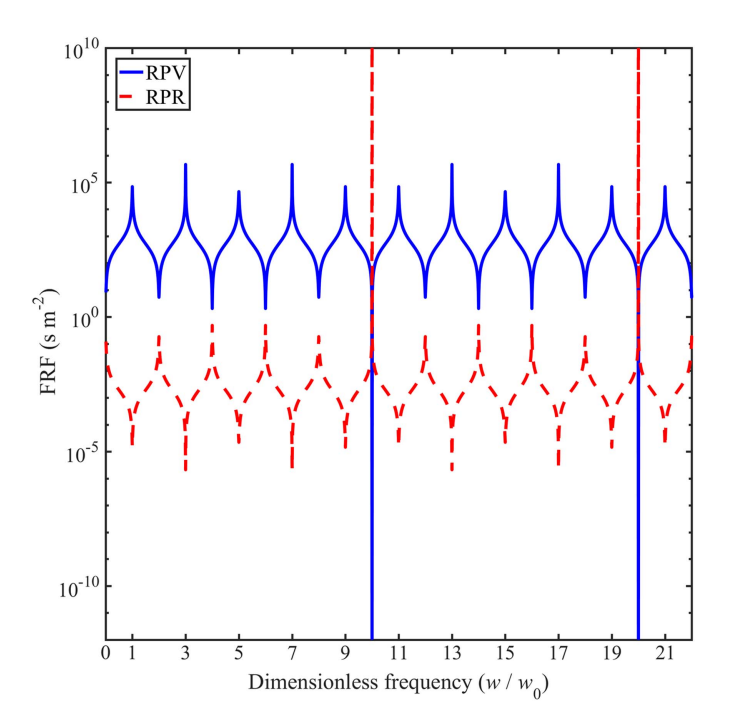


Fig. 10. Comparison of FRFs of RPV and RPR systems with measurement at $x_M = L$ and a leak at $x_l = 3/5L$.

Relation of Bragg Resonance to the Method by Gong et al. (2013)

A recently developed leak detection method by Gong et al. (2013) uses only the first three resonant peaks to locate leaks. This means that this method does not require a large frequency bandwidth for accurate leak detection, a feature that is usually preferred in practice. In fact, the lower the number of resonant frequency is required, the fewer requirements on the sharpness of the generated transient wave are imposed, which is easier to deliver in practice (e.g., slower valve maneuver). The interesting part of this method and its relation to the current work is that Gong et al. (2013) reported that the method fails when leaks are located near the boundaries, or close to the pipe middle point. To understand why the method fails, one needs to briefly review the principle of the leak detection method by Gong et al. (2013). The method uses a characteristic equation of the resonant peak amplitude $\overline{h_c}(\overline{Z_v}, \overline{Z_L}, x_l^*, w_m)$, which is valid at every resonant frequency w_m and depends on three unknowns: $\overline{Z_v}$, $\overline{Z_L}$, and x_l^* as follows (Gong et al. 2013):

$$\overline{h_c}(\overline{Z_v}, \overline{Z_L}, x_l^*, w_m) = \frac{\overline{Z_v}}{1 + \overline{Z_L}(1 - \cos(\pi x_l^* w_m))}$$
(36)

If Eq. (36) is applied to the first three resonant peaks, then one can solve for the three unknowns given the three equations. Note that the system of three equations—three unknowns provides a unique solution provided that the equations are independent. The violation of this condition is what causes the failure of the method when the leak induces the same effect on the used harmonics. Fig. 11(a) gives the first three resonant peaks of a FRF of a RPV with a leak located at the middle of the pipe, and Fig. 11(b) gives the first three harmonic functions. Notice that the first three resonant peaks have the same values. This is understood because, at the middle of a RPV system, the harmonic functions have the same magnitudes. In this case, the system of three equations—three unknowns reduces to a system of one equation—three unknowns

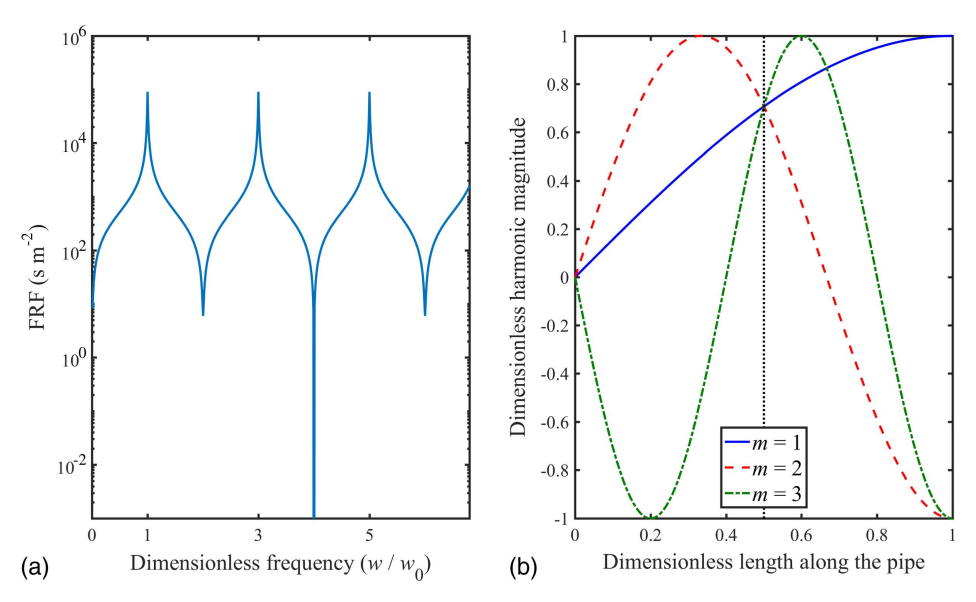


Fig. 11. (a) First three resonant peaks of a FRF of a RPV with a leak located at the middle of the pipe and measurement at $x_M = L$; and (b) first three harmonic functions.

because applying Eq. (36) to the first three resonant frequencies gives the same value. Fig. 11(b) shows that this is also the case at the pipe boundaries. Therefore, the method by Gong et al. (2013) is found to be sensitive when the harmonic amplitudes of the first three modes are close to each other.

Conclusions

Wave-leak interaction was studied for a simple case of a frictionless pipe connected to a reservoir at the upstream boundary and to a valve at the downstream boundary. The theoretical analysis shows that, depending on the leak location, some of the pipe harmonics experience special resonance behavior. The conditions of these special cases are similar to the Bragg resonance conditions. Unlike blockages, which were studied previously by the authors, a leak has a vanishingly small length (generally modeled as a point). If the previous blockage work is extended for the leak case, it would require an infinitesimal wavelength (i.e., infinite frequency). Yet, leak-imposed patterns are known to occur for finite wavelengths. Therefore, this work proposes a novel mechanism that is responsible for leak-induced Bragg resonance and explains the transientbased leak-induced patterns that are available in the literature (both experimentally and numerically) from a new and explicit point of view.

In particular, if the leak is located at a maximum pressure node of a given harmonic, this latter experiences Bragg-type resonance of maximum reflection. The reason is that, although the leak is located at maximum pressure node, it induces severe damping, and therefore, waves propagating at a frequency similar or multiple of that given harmonic experience maximum reflection. By consequences, this emphasizes the leak location and size in the FRF, where the location of the leak is determined from the possible maximum pressure nodes and the size of the leak is determined from the lowest magnitude observed in the FRF.

On the other hand, if a leak is located at a zero pressure node of a given harmonic, this latter experiences Bragg-type resonance of maximum transmission. The reason is that, although the leak is located at zero pressure, it no longer has any effect on that particular harmonic, and therefore, wave propagation at a frequency similar or multiple of that given harmonic does not experience any reflection.

(The impedance at the leak for those waves appears to be the same as the impedance of the pipe.) In return, this emphasizes the leak location in the FRF, where the location of the leak is determined from the possible zero pressure nodes of the mode having the highest magnitude in the FRF.

The current work is based on either the boundaries of the systems are known and controllable, or (if not controllable) the FRF of the intact case is known. Therefore, in practice, if a real system is complex, then it is already challenging to any available leak detection method. However, according to the theory of Bragg resonance, if the FRF is obtained at different measurement locations, it should be possible to obtain more insights on the system. This is an ongoing research work, and it is out of the scope of this paper. In fact, the authors have already started field work in Hong Kong to validate the use of Bragg resonance at field scale.

Appendix. Details on Governing Equations and Boundary Conditions

Eq. (3) is derived from Eq. (2) as follows:

$$\frac{\partial^2 H}{\partial t^2} - a^2 \frac{\partial^2 H}{\partial x^2} = 0 \tag{37}$$

If $H = \tilde{H}(x, w) \exp(iwt)$, then

$$\frac{\partial^{2} [\tilde{H}(x, w) \exp(iwt)]}{\partial t^{2}} - a^{2} \frac{\partial^{2} [\tilde{H}(x, w) \exp(iwt)]}{\partial x^{2}} = 0$$
 (38)

$$\Rightarrow \tilde{H}(x,w) \frac{\partial^2 [\exp(iwt)]}{\partial t^2} - a^2 \frac{\partial^2 [\tilde{H}(x,w)]}{\partial x^2} \exp(iwt) = 0 \quad (39)$$

$$\Rightarrow \tilde{H}(x,w)[-w^2\exp(iwt)] - a^2 \frac{d^2[\tilde{H}(x,w)]}{dx^2}\exp(iwt) = 0 \quad (40)$$

$$\Rightarrow \tilde{H}(x,w)[-w^2\exp(iwt)] - a^2\frac{d^2[\tilde{H}(x,w)]}{dx^2}\exp(iwt) = 0 \quad (41)$$

$$\Rightarrow -w^2 \tilde{H}(x, w) - a^2 \frac{d^2 \tilde{H}(x, w)}{dx^2} = 0 \tag{42}$$

$$\Rightarrow \frac{d^2 \tilde{H}(x, w)}{dx^2} + \underbrace{\left(\frac{w}{a}\right)}_{k^2} \tilde{H}(x, w) = 0$$
 (43)

Details on Eq. (5) are as follows:

$$\tilde{H}_1 = \tilde{H}_2 = H_L$$

$$\tilde{Q}_1 = \tilde{Q}_2 + Q_L \Leftrightarrow \frac{gA}{iw} \frac{d\tilde{H}_1}{dx} = \frac{gA}{iw} \frac{d\tilde{H}_2}{dx} + s\tilde{H}_2 \quad \text{at } x = 0 \quad (44)$$

The water-hammer momentum equation gives

$$\frac{\partial Q}{\partial t} = gA \frac{\partial H}{\partial x} \Rightarrow \int \frac{\partial Q}{\partial t} dt = Q = \int gA \frac{\partial H}{\partial x} dt \qquad (45)$$

If $H = \tilde{H}(x, w) \exp(iwt)$, then

$$Q = \tilde{Q}(x, w) \exp(iwt) = \int gA \frac{\partial H}{\partial x} dt$$

$$= gA \left[\frac{1}{iw} \frac{d\tilde{H}(x, w)}{dx} \right] \exp(iwt) \Rightarrow \tilde{Q}(x, w) = \frac{gA}{iw} \frac{d\tilde{H}(x, w)}{dx}$$
(46)

Because the leak is modeled by the linearized orifice equation, which is given by

$$Q_l = sH \tag{47}$$

Finally

$$\tilde{Q}_1 = \tilde{Q}_2 + Q_L \Leftrightarrow \frac{gA}{iw} \frac{d\tilde{H}_1}{dx} = \frac{gA}{iw} \frac{d\tilde{H}_2}{dx} + s\tilde{H}_2 \quad \text{at } x = 0 \quad (48)$$

Eq. (7) gives a system with four equations and four unknowns. When solved for H_1^{ref} , it gives Eq. (8). Eq. (11) is the derivative of Eq. (12). When the derivative is zero, it gives the extremum. The conditions in Eqs. (12) and (13) come from the found extremum. The sign of the second derivative of Eq. (10) will inform which extremum is maximum or minimum, which in return identifies the maximum or minimum reflection.

Acknowledgments

This study was supported by the Hong Kong Research Grant Council (Project Nos. T21-602/15R and 16208618). The authors thank Dr. D. A. McInnis for the technical and editorial suggestions.

Notation

The following symbols are used in this paper:

 $A = pipe area (m^2);$

 $\bar{A}_L = \text{modified leak size (m}^2);$

a = acoustic wave speed in water (m s⁻¹);

 $g = \text{gravity (m s}^{-2});$

H = pressure head (m);

 H_i^{ref} = reflected pressure amplitude at pipe region j (m);

 H_i^{tr} = transmitted pressure amplitude at pipe region j (m);

 H_L = pressure head at the leak (m);

 \bar{H}_L = mean pressure head at the leak (m);

 $\tilde{H}(x, w)$ = amplitude of the harmonic pressure head (m);

 H_0 = initial pressure in the pipe (m);

 \bar{h}_c = characteristic function;

 $i = \sqrt{-1}$;

j = pipe number;

 $k = \text{wave number } (\text{m}^{-1});$

L = pipe length (m);

 M_{u-d} = transfer matrix entrance from upstream location to downstream location;

 M_{u-x_M} = transfer matrix entrance from upstream location to measurement location (s m⁻²);

m = resonant mode number;

 m_i , m_{i2} , m_2 = integers/counters;

 $n, n_0 = \text{integers/counters};$

 $Q = \text{flow rate } (\text{m}^3 \text{ s}^{-1});$

 Q_L = flow at the leak (m³ s⁻¹);

 \bar{Q}_L = mean flow rate at the leak (m³ s⁻¹);

 R_c = squared norm of the normalized reflection amplitude (s² m⁻⁴);

 R_{mL} = damping function of the *m*th mode (m²);

 $s = leak size (m^2);$

t = time (s);

 $w = \text{angular frequency (rad s}^{-1});$

 $w_m = m$ th resonant frequencies in the blocked pipe case (rad s⁻¹);

 $w_m^T = \text{Bragg resonance frequency of maximum}$ reflection (rad s⁻¹);

 w_n^R = Bragg resonance frequency of maximum reflection (rad s⁻¹);

x = axial coordinate (m);

 $x_l = \text{leak location (m)};$

 x_I^* = dimensionless leak location (m);

 x_M = measurement location (m);

 $Z = \text{pipe characteristic impedance (s m}^{-2});$

 Z_L = leak impedance (s m⁻²);

 $\bar{Z}_L = \text{modified leak impedance (s m}^{-2});$

 $\bar{Z}_v = \text{modified valve impedance (s m}^{-2});$

 $\lambda =$ probing wavelength (m); and

 Υ = frequency response function (s m⁻²).

References

Bragg, W. H., and W. L. Bragg. 1913. "The reflection of X-rays by crystals." *Proc. R. Soc. London, Ser. A* 88 (605): 428–438. https://doi. org/10.1098/rspa.1913.0040.

Brunone, B. 1999. "Transient test-based technique for leak detection in outfall pipes." *J. Water Resour. Plann. Manage.* 125 (5): 302–306. https://doi.org/10.1061/(ASCE)0733-9496(1999)125:5(302).

Chaudhry, M. H. 2014. Applied hydraulic transients. 3rd ed. New York:

Covas, D., H. Ramos, and A. B. de Almeida. 2005. "Standing wave difference method for leak detection in pipeline systems." J. Hydraul. Eng. 131 (12): 1106–1116. https://doi.org/10.1061/(ASCE)0733-9429 (2005)131:12(1106).

Covas, D. I., H. M. Ramos, and A. B. de Almeida. 2008. "Closure to 'Standing wave difference method for leak detection in pipeline systems' by Dídia IC Covas, Helena M. Ramos, and António Betâmio de Almeida." J. Hydraul. Eng. 134 (7): 1029–1033. https://doi.org/10.1061/(ASCE)0733-9429(2008)134:7(1029).

Ferrante, M., and B. Brunone. 2003a. "Pipe system diagnosis and leak detection by unsteady-state tests. I: Harmonic analysis." Adv.

- Water Resour. 26 (1): 95–105. https://doi.org/10.1016/S0309-1708(02) 00101-X.
- Ferrante, M., and B. Brunone. 2003b. "Pipe system diagnosis and leak detection by unsteady-state tests. II: Wavelet analysis." *Adv. Water Resour.* 26 (1): 107–116. https://doi.org/10.1016/S0309-1708(02) 00102-1.
- Ferrante, M., B. Brunone, and S. Meniconi. 2007. "Wavelets for the analysis of transient pressure signals for leak detection." *J. Hydraul. Eng.* 133 (11): 1274–1282. https://doi.org/10.1061/(ASCE)0733-9429 (2007)133:11(1274).
- Ghidaoui, M. S. 2004. "On the fundamental equations of water hammer." *Urban Water J.* 1 (2): 71–83. https://doi.org/10.1080 /15730620412331290001.
- Gong, J., M. F. Lambert, A. R. Simpson, and A. C. Zecchin. 2013. "Single-event leak detection in pipeline using first three resonant responses." J. Hydraul. Eng. 139 (6): 645–655. https://doi.org/10.1061/(ASCE)HY.1943-7900.0000720.
- Lee, P., J. Tuck, M. Davidson, and R. May. 2017. "Piezoelectric wave generation system for condition assessment of field water pipelines." J. Hydraul. Res. 55 (5): 721–730. https://doi.org/10.1080/00221686 .2017.1323805.
- Lee, P. J., M. F. Lambert, A. R. Simpson, J. P. Vítkovský, and J. Liggett. 2006. "Experimental verification of the frequency response method for pipeline leak detection." *J. Hydraul. Res.* 44 (5): 693–707. https://doi. org/10.1080/00221686.2006.9521718.
- Lee, P. J., J. P. Vítkovský, M. F. Lambert, A. R. Simpson, and J. A. Liggett. 2005a. "Frequency domain analysis for detecting pipeline leaks." *J. Hydraul. Eng.* 131 (7): 596–604. https://doi.org/10.1061/(ASCE) 0733-9429(2005)131:7(596).
- Lee, P. J., J. P. Vítkovský, M. F. Lambert, A. R. Simpson, and J. A. Liggett. 2005b. "Leak location using the pattern of the frequency response diagram in pipelines: A numerical study." *J. Sound Vib.* 284 (3–5): 1051–1073. https://doi.org/10.1016/j.jsv.2004.07.023.
- Louati, M., M. S. Ghidaoui, S. Meniconi, and B. Brunone. 2018. "Bragg-type resonance in blocked pipe system and its effect on the eigenfrequency shift." *J. Hydraul. Eng.* 144 (1): 04017056. https://doi.org/10.1061/(ASCE)HY.1943-7900.0001383.

- Louati, M., S. Meniconi, M. S. Ghidaoui, and B. Brunone. 2017. "Experimental study of the eigenfrequency shift mechanism in a blocked pipe system." *J. Hydraul. Eng.* 143 (10): 04017044. https://doi.org/10.1061/(ASCE)HY.1943-7900.0001347.
- Maloney, C. A. 1973. "Locating cable faults." IEEE Trans. Ind. Appl. IA-9 (4): 380–394. https://doi.org/10.1109/TIA.1973.349965.
- Mei, C. C. 1985. "Resonant reflection of surface water waves by periodic sandbars." J. Fluid Mech. 152 (3): 315–335. https://doi.org/10.1017 /S0022112085000714.
- Nixon, W., and M. S. Ghidaoui. 2007. "Numerical sensitivity study of unsteady friction in simple systems with external flows." *J. Hydraul.* Eng. 133 (7): 736–749. https://doi.org/10.1061/(ASCE)0733-9429 (2007)133:7(736).
- Nixon, W., M. S. Ghidaoui, and A. A. Kolyshkin. 2006. "Range of validity of the transient damping leakage detection method." *J. Hydraul. Eng.* 132 (9): 944–957. https://doi.org/10.1061/(ASCE)0733-9429(2006) 132:9(944).
- Sattar, A. M., and M. H. Chaudhry. 2010. "Leak detection in pipelines by frequency response method." Supplement, *J. Hydraul. Res.* 46 (S1): 138–151. https://doi.org/10.1080/00221686.2008.9521948.
- Tijsseling, A. S., and A. Vardy. 2017. "Some intriguing aspects of boundary conditions in water hammer." In E-Proc., 37th IAHR World Congress. London: Taylor and Francis.
- Vítkovský, J. P., and P. J. Lee. 2008. "Discussion of 'Standing wave difference method for leak detection in pipeline systems' by Dídia IC Covas, Helena M. Ramos, and António Betâmio de Almeida." *J. Hydraul. Eng.* 134 (7): 1027–1029. https://doi.org/10.1061/(ASCE)0733-9429(2008) 134:7(1027).
- Wang, X., and M. S. Ghidaoui. 2018. "Pipeline leak detection using the matched-field processing method." J. Hydraul. Eng. 144 (6): 04018030. https://doi.org/10.1061/(ASCE)HY.1943-7900.0001476.
- Wang, X. J., M. F. Lambert, A. R. Simpson, J. A. Liggett, and J. P. Vítkovský. 2002. "Leak detection in pipelines using the damping of fluid transients." *J. Hydraul. Eng.* 128 (7): 697–711. https://doi.org/10.1061/(ASCE)0733-9429(2002)128:7(697).
- Wylie, E. B., and V. L. Streeter. 1993. *Fluid transients in systems*. Englewood Cliffs, NJ: Prentice Hall.